Analyzing the operational performance of the hydrological models in an alpine flood forecasting system

Achleitner, S ; Schöber, J ; Rinderer, M ; Leonhardt, G ; Schöberl, F ; Kirnbauer, R ; Schönlaub, H

Abstract: During recent years a hybrid model has been set up for the operational forecasting of flood discharges in the 6750 km2 Tyrolean part of the River Inn catchment in Austria. The catchment can be characterized as a typical alpine area with large variations in altitude. The paper is focused on the error analysis of discharge forecasts of four main tributary catchments simulated with hydrological water balance models. The selected catchments cover an area of 2230 km2, where the non-glaciated and glaciated parts are modeled using the semi-distributed HQsim and the distributed model SES, respectively. The forecast errors are evaluated as a function of forecast lead time and forecasted discharge magnitude using 14 events from 2007 to 2010. The observed and forecasted precipitation inputs were obtained under operational conditions. The mean relative bias of the forecasted discharges revealed to be constant with regard to the forecast lead time, varying between 0.2 and 0.25 for the different catchments. The errors as a function of the forecasted discharge magnitude showed large errors at lower values of the forecast hydrographs, where errors decreased significantly at larger discharges being relevant in flood forecasting.

DOI: https://doi.org/10.1016/j.jhydrol.2011.07.047

Analyzing the operational performance of the hydrological models in an alpine flood forecasting system

S. Achleitner[1], J. Schöber[2,3], M. Rinderer[4], G. Leonhardt[5], F. Schöberl[3], R. Kirnbauer[6], H. Schönlaub[7]

[1] Unit of Hydraulic Engineering, University of Innsbruck, Austria

[2] alpS – Centre for Climate Change Adaptation Technologies, Innsbruck, Austria

[3] Institute of Geography, University of Innsbruck, Austria

[4] Hydrology and Climate Unit, Department of Geography, University of Zurich, Switzerland

[5] Unit of Environmental Engineering, University of Innsbruck, Austria

[6] Institute of Hydraulic Engineering and Water Resources Management, Vienna University of Technology, Austria

[7] TIWAG – Tiroler Wasserkraft AG, Austria

Correspondence to: Stefan Achleitner (Unit of Hydraulic Engineering, University of Innsbruck, Austria, Technikerstr. 13, 6020 Innsbruck, stefan.achleitner@uibk.ac.at)

Abstract

During recent years a hybrid model has been set up for the operational forecasting of flood discharges in the 6750 km^2 Tyrolean part of the River Inn catchment in Austria. The catchment can be characterized as a typical alpine area with large variations in altitude. The paper is focused on the error analysis of discharge forecasts of four main tributary catchments simulated with hydrological water balance models. The selected catchments cover an area of 2230 km^2, where the non-glaciated and glaciated parts are modeled using the semi-distributed HQsim and the distributed model SES, respectively.

The forecast errors are evaluated as a function of forecast lead time and forecasted discharge magnitude using 14 events from 2007 to 2010. The observed and forecasted precipitation inputs were obtained under operational conditions. The mean relative bias of the forecasted discharges revealed to be constant with regard to the forecast lead time, varying between 0.2 and 0.25 for the different catchments. The errors as a function of the forecasted discharge magnitude showed large errors at lower values of the forecast hydrographs, where errors decreased significantly at larger discharges being relevant in flood forecasting.

1 Introduction

The work presented in this paper deals with the evaluation of the flood forecasting performance of four representative tributaries discharging to the River Inn in Tyrol (a western province of Austria). These catchments are part of the flood forecasting system "HoPI" (**Ho**chwasser**p**rognose für den Tiroler **I**nn). The total River Inn catchment covers an area of 6750 km^2 along the 200 km-long stretch of the river Inn between the Engadin (Switzerland) and Bavaria (Germany). The selected hydrologically modelled tributary catchments account for 2230 km^2 (33%) of the total catchment.

Runoff from tributaries to the River Inn is dominated by snow melt and ice melt from glaciated parts of the basin. Therefore the hydrological models of the tributaries are, depending on the catchment, composed of (1) the Snow- and Icemelt Model SES for the hydrology of glaciated catchments (Asztalos et al., 2007; Blöschl et al., 1991a; Blöschl et al., 1991b; Schöber et al., 2010a) and (2) HQsim for the hydrology of non-glaciated catchments or catchment parts (Achleitner et al., 2009; Kleindienst, 1996). The River Inn itself is modeled with the Flux$^{DSS/DESIGNER}$/FLORIS^{2000} (Reichel et al., 2000) a 1D hydraulic model. Forecasted discharges downstream are provided as input to the forecast model for Bavaria, Germany (Ehret et al., 2009).

The HQsim and SES hydrological models are semi-distributed and distributed water-balance models, respectively. Other examples of forecasting systems in alpine area using water balance models include Jasper et al. (2002) or Verbunt et al. (2007), to

list two Swiss examples, and the Kamp model in Lower Austria (Blöschl et al., 2008). The use of water balance models is a vital part, since the continuously obtained system states (e.g. soil saturation, snow cover) have a significant impact on the runoff formation (Marchi et al., 2010; Schöber et al., 2010b).

In the evaluation of the flood forecasting performance of past flood events the meteorological input uncertainty is thereby considered to be the largest source of uncertainty (Rossa et al., 2010a). For the continuous simulations hourly meteorological station data provided in real time was utilized. For the forecast period, the results of the meteorological forecast tool INCA (Integrated Nowcasting through Comprehensive Analysis) (Haiden et al., 2010) is used as primary input. All input data used in the investigation remained as provided under operational conditions, having the full spectrum of possible errors included. The focus was on the quantification of errors in the produced discharge forecast. The errors were evaluated as a function of the forecast lead time and the forecasted discharge magnitude.

2 Methods

2.1 Model description

2.1.1 Catchments and meteorological Data

For this study, we analyzed four different tributary catchments which are representative for the main landscape types of the Inn catchment. Figure 1 provides an overview on the location and extend of the four from totally 49 tributary catchments. The difference in elevation of the model area ranges from 3762 m to a minimum elevation of 500 m at the boarder to Germany. In 2009 the Austrian Inn catchment had a glaciated area of roughly 200 km² (estimated from a Landsat Image of August 2009). The flow from the glaciated headwaters of the Inn catchment is modeled using SES model (see details below). Two of the considered tributaries (Ötztal and Sanna) are influenced by glaciated headwaters (see Figure 1). The largest tributary, Ötztaler Ache, has four different SES model-areas included, and the runoff of each model serves as input for the routing routine of the HQsim model (see details below).

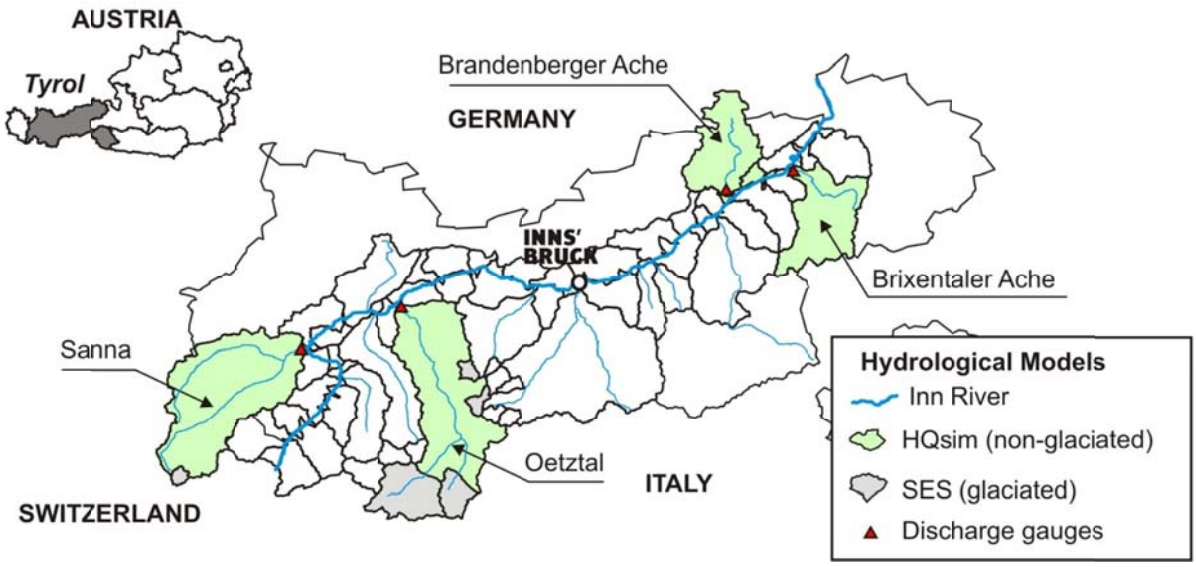

Figure 1: Total catchment of the Tyrolean River Inn with its tributary catchments. The four catchments assessed in this paper are marked in green (non-glaciated parts) and gray (glaciated parts)

The main reason for the selection of the model areas was the availability of gauge measurements (see Figure 1) and the location of the catchments – one of the selected watersheds is located in the western part of the country, two are located south of the Inn valley and one is situated north of the Inn valley. Table 1 summarizes the main catchment features including the estimated ranges of rainfall-runoff concentration times during observed medium and large storm events.

Table 1: Characteristics of the investigated tributary catchments

	Area	Elevation [m.a.s.l]		Glaciation		tc
	[km^2]	min	max	[km^2]	[%]	[h]
Brandenberger Ache	280	508	2250	0	0	7-14
Brixentaler Ache	330	500	2466	0	0	3-8
Sanna	727	769	3397	9	1,2	3-8
Oetztaler Ache	893	673	3762	90	10	5-15

tc…Concentration time

Catchments in the north-western and south-eastern parts of the Inn catchment are affected differently by the predominantly western frontal weather system. Comparable meteorological conditions can be expected for the catchment areas of the Brandenberger Ache and the Brixentaler Ache, and differences in runoff may be due to differing geology. In contrast, the glaciated Sanna or Ötztaler Ache

catchments show differing runoff regimes and, consequently, different types of floods.

In the operational mode, the flood warning system is generating forecasts on an hourly basis using remotely transmitted meteorological and hydrological data. Both data sets are provided by different institutions and are assembled at the Tyrolean hydrological service. Hourly meteorological forecast sets are obtained from the weather prediction tool INCA. Precipitation and temperature data from 74 meteorological weather stations serve as primary input of the HQsim and SES hydrological models. Precipitation data provided by observation or by the forecast model is spatially interpolated onto a 5 km x 5 km spatial grid. Temperature stations at various elevations are used to calculate the base temperature and associated lapse rates for different regions of the Inn catchment (Rinderer et al., 2008). The SES energy balance model requires additional measurements of global radiation, relative humidity and wind speed from 15 stations.

Observed discharge data, available for selected tributary catchments, is provided online for output-correction. The output-corrected discharges serve as input for the hydraulic model of the Inn River, where the output-correction itself is limited to the first hours of the forcast period.

2.1.2 HQsim

For non-glaciated areas the HQsim model (Kleindienst, 1996) is applied, which is a semi-distributed water balance model based on hydrological response units (HRU's or hydrotopes). For the purpose and spatial scale of the flood-forecasting system HOPI, soil type, aspect and elevation have been determined to be most relevant to delineate these hydrotopes. The map of soil types was taken from the Hydrological Atlas of Austria (BMLFUW, 2007). In addition further hydrologically relevant characteristics, namely vegetation attributes, soil depth and slope angle, are then assigned to these hydrotopes. These attributes are derived either from a digital elevation model (resolution: 50m x50m) or from remotely sensed data (Corine Land Cover (Bossard et al., 2000)).

For each of these hydrotopes runoff generation is modeled separately, using spatially distributed precipitation inputs. Dependent on the air temperature, which is calculated for the mean elevation of each hydrotope, the precipitation is either falling as rain,

rain-snow mixture or as snow. A portion is kept in the tree canopy but the larger fraction reaches the ground. Snowmelt is modeled using a modified degree-day factor approach (Hock, 1999) additionally accounting for exposition, slope and inclination of the sun. The concept of “cold content” defined as the sum of negative temperature accumulated over previous days, is used to parameterize the energy balance of the snow cover and simulate the delayed onset of snowmelt once air temperature rises above the melting point. Potential evapotranspiration is simulated based on Hamon (1963) resulting in lower values during winter and higher values during summer time. Modeling of surface runoff generation within each hydrotope is based on the contributing area concept: The fraction of area contributing to surface runoff is a function of soil water content and thus changing in time. Soil water content and associated subsurface flow in the unsaturated zone is simulated using the Mualem-van Genuchten approach (van Genuchten, 1980). The saturated zone is simulated using a linear storage to calculate outflow, which supplements to stream flow discharge in the nearest stream channel. The runoff concentration between a HRU and its nearest channel reach is simulated separately for surface flow, and subsurface flow. The concentration time of the surface flow is calculated according to Morgali and Linsley (1965)

The delayed routing of subsurface flow is described as a function of the hydraulic conductivity and the HRU’s distance to the channel reach. Once the water has reached the channel, it is routed downstream using an approach based on Rickenmann (1996). Man-made intakes or reservoirs can be defined and modeled in each channel segment.

2.1.3 SES

The snow and glacier melt model (SES) is a fully distributed energy and water balance model which calculates the flow of the glaciated catchments in a spatial resolution of 50 m x 50 m. The model calculates the accumulation of snow and firn and the snow, firn, and ice melt for each grid element at hourly intervals on basis of energy balance equation. As short-wave radiation is the dominating source of the melt energy, seasonal and daily changes of the albedo (as a consequence of progressing metamorphosis of the snow pack and diurnal variations of the albedo depending on the reflectivity of snow for changing irradiation angle) were taken into

account in the modeling approach. Therefore, the decrease of albedo during melt is not modelled as a function of time (e.g., the aging curve approach of the US Army Corps of Engineers (1956)), but rather as a function of the total energy input the snowpack has received. A modified version of the approach of Trofimova (1970) is used (Asztalos, 2004). Consequently, hourly air temperature, precipitation, relative humidity, wind speed and global radiation are used as input. Cloudiness is estimated from the observed global radiation and astronomically possible radiation (Kasten and Czeplak, 1980). To simulate the internal heat and mass fluxes in the snow pack, an approach based on the concepts of water retention and cold content is used (Braun, 1985). Precipitation and melt water is cumulated for the four types of areas on the glacier with temporally changing extents (non-glaciated, snow free, firn and snow) and routed via four parallel linear reservoirs (Nash, 1960). An additional Nash cascade covering the subsurface flow completes the routing systems.

2.2 Model Calibration

The hydrological models were calibrated using observed stream flow gauge data (see gauge locations in Figure 1) and remotely sensed snow patterns. Flow measurements and meteorological input data were continuously available for all catchments since October 1994. The whole data set was divided into a calibration period and a validation period. The models were tested for correct representation of seasonal discharge variation as well as large flow events. A semi-automatic approach was used for splitting a continuous hydrograph into single events (Achleitner et al., 2009). An event was thereby defined as a flow series that exceeded a catchment-specific discharge limit (e.g. the one-year return period). As a second boundary, a minimum low-flow period between two events was defined, which allowed two consecutive peaks to be treated as one event in the evaluation. The tuned model parameters of both models are summarized in **Table** 2.

Table 2: HQsim and SES parameters used in the calibration (adopted from Achleitner et al. (2009) and Schöber et al.(2010a))

HQsim - Parameters

Parameter	Unit	Description
cap1	-	Parameter for the calculation of the flow contributing area
cap2	-	Parameter for the calculation of the flow contributing area
mvga	-	Mualem Van-Genuchten parameter a
mvgks	mm/d	Saturated hydraulic permeability
mvgm	-	Mualem Van-Genuchten parameter m
sd	mm	Depth of the unsaturated flow zone
usd	-	Unsatured drainage percentage - fraction that is diverted to the groundwater storage
sntmem	d	Maximum days of snow temperature memory
sntmin	°C	Lower limit of snow temperature
snmfmin	mm/°C/d	Minima day degree factor
snmfmax	mm/°C/d	Maxima day degree factor
tsrmin	°C	Lower temperature für snow/rain transition
tsrmax	°C	Upper temperature für snow/rain transition
snowcorr	%	Correction factor for measurement errors during snowfall

SES - Parameters

Parameter	Unit	Description
ans	-	Albedo of new snow
aos	-	Albedo of old snow
afirn	-	Albedo of firn
aice	-	Albedo of ice
ghf	W/m²	Ground heat flux
twsrmin	°C	Lower wet bulb temperature für snow/rain transition
twsrmax	°C	Upper wet bulb temperature für snow/rain transition
snowcorr	%	Correction factor for measurement errors during snowfall
slpmin	°	Redistribution of snow - slope min
slpmax	°	Redistribution of snow - slope max
snow, ksno	-, h	Nash Cascade parameters for the snow covered area
nfirn, kfirn	-, h	Nash Cascade parameters for the firn covered area
nice, kice	-, h	Nash Cascade parameters for the glaciers
nng, kng	-, h	Nash Cascade parameters for the non-glaciated area
nsoil, ksoil	-, h	Nash Cascade parameters for the soil/subsurface flow

The modeled discharges have been evaluated on basis of single flood events and long-term discharge series. The bias (multiplicative) of the discharge volume was used, defined as the ratio between simulated and observed discharge volumes. Furthermore, each of the flood events was then evaluated separately for indicators such as measured and simulated peak flows (Q_{MAX-M} [m³/s] vs. Q_{MAX-S} [m³/s]), the temporal shift of the peak flow (ΔT [h]) and the Nash–Sutcliffe Efficiency (Nash and Sutcliffe, 1970) of the event.

In addition, a separate verification of the simulations was made using the distributed snow cover as a reference (Schöber et al., 2010a). The glaciated parts of the

catchments were investigated in depth using different remote sensing sources such as Landsat (Dozier and Marks, 1987) to detect snow depletion patterns. The method allows only a verification of the spatial distribution of snow on glaciers but not to estimate the total stored amount of snow water equivalent (Arheimer et al., 2010). This verification of the simulated spatial extent of the snow cover on glaciers was made at the end of a 15-year period of SES-simulation without any state corrections. The overall agreements achieved between observed and simulated snow cover ranged from 68% to 88% in the individual glaciated catchments. For the remaining non-glacierized catchments, which are simulated using HQsim, similar investigations of spatial snow cover patterns at the end of the winter season have been made as well. In contrast to the glacierized catchments, the verification was made visually for specific years. Considering the scale of the hydrotopes given, Landsat as well as MODIS data (Hall et al., 1995) were used to validate the extent of the snow cover.

2.3 Forecasting

2.3.1 Meteorological forecast data

In the forecast period (lead time up to 48 hours) the models are driven by the INCA (Integrated Nowcasting through Comprehensive Analysis) meteorological forecasts provided by the Austrian Meteorological Office (ZAMG) (see Haiden et al.(2010)). Therein the precipitation, temperature, global radiation, humidity and wind speed are available on a 1 km grid.

Errors in numerical weather prediction (NWP) models (lead time up to 6 hours) are usually not significantly smaller than those observed for 12 to 24 hours lead time (Golding, 1998; Haiden et al., 2010). Thus, in INCA the forecast is a mix of nowcasting and numerical weather prediction modeling for the first 6 hours ahead such as found as well in Golding (2000). For the Austrian region, the limited area model ALADIN (Wang et al., 2006) is combined with surface station observations, radar data and elevation data to produce improved meteorological short-term forecasts.

The spatial resolution of INCA (1 km compared to 10 km in the ALADIN model) enables a more detailed consideration of the topography, which is especially important in mountainous areas. The density of stations in the study area in

elevations up to 1500m a.s.l. is considered sufficient. At higher elevations, the station density is less than optimum (Haiden et al., 2010). In elevated alpine locations, stations are rare and only located at a few remote locations.

As a second source for the precipitation field analysis, observations obtained by the Austrian Radar Network were used in INCA. An improved quantitative precipitation estimation when using radar data is reported by Rossa et al. (2010b). One of the radar devices used is located in the center of the Inn catchment. But even situated at an elevation of 2000 m.a.s.l., radar signals of selected parts of the Inn-catchment can not be processed due to shading effects of the mountainous topography. The radar data is climatologically scaled (calibrated) for ground gauge stations using monthly precipitation sums. Secondly the obtained precipitation fields are combined linearly using climatological scaling factors obtained earlier (Komma et al., 2007).

The remaining parameters are also derived at a grid level of 1 km spacing. The temperature field is based on the interpolation of station data and combined with the first ALADIN forecast used as a first guess for the spatial distribution. In case of cloudiness, satellite images are used as additional data source. The derived cloudiness distribution is crosschecked with the spatial distribution of rainfall (Haiden et al., 2010).

2.3.2 Runoff forecasting and evaluation

The INCA data sets described above are the driving elements in the forecast period and allow a forecast lead time of up to 48 hours in the hydrological simulations. The nominal forecast time T_0 is defined as the latest point in time where at least 80% of the precipitation stations and 80% of the temperature stations are providing current data via the online network. Using this threshold, a simulation run between the last and the current T_0 is considered to have sufficient input data to reliably calculate a new model state. The forecasted discharge, simulated in the following using INCA as the driving meteorological input, is based on this initial model states. Still, the online available and transmitted data have an impact not only on the current model state, but these data are also the basis for the INCA data set. Due to the given tight time intervals at which INCA data is provided (15 min time steps for precipitation forecasts; 1h time steps for forecasts of remaining parameters) only the data

transmitted close to real time is considered in the INCA analysis and consequently in the forecast.

The forecasted and measured datasets used in this paper originate from the online operation period of the forecasting system between 2007 and 2010. Thus the data includes all errors that are typically introduced during an online operation. For the evaluation of the forecast quality, totally 14 events were identified which caused increased discharge in one or more of the considered hydrological catchments. The HoPI system allows recalculation of previous time periods with locally stored INCA data sets in order to mimic conditions during online operation. The investigations deliberately excluded the use of already implemented model output correction routines in order to evaluate the model performance based on different input data only.

The forecasts obtained for the 14 events were analyzed for errors occurring in the rainfall itself and the resulting discharge from the catchment. The forecast of the mean forecasted areal precipitation (r_f) was compared to the mean observed precipitation (r_o), knowing that the measured rainfall does not necessarily represent the ground truth since the online obtain datasets remained uncorrected. To consider different forecast horizons, the cumulated forecasted and observed precipitations (RF and RO) are used.

$$R_{F,TF} = \sum_{i=1}^{TF} r_{F,i} \qquad \text{Equation 1}$$

The evaluation of forecasted rainfall was made for the cumulated precipitation at different levels of forecast horizons. Consequently, forecasted discharges (Q_{SF}) were compared to both, measured discharge (Q_M) and simulated discharge using rainfall measurements as input (Q_{S0}). In the evaluation the Nash Sutcliffe Efficiency (NSE) (Nash and Sutcliffe, 1970) was applied to evaluate the fit of the hydrographs. Further, the relative bias was used as an indicator to relate discharge difference to the level of discharge.

$$NSE = 1 - \frac{\sum_{i=1}^{N} \left(Q_{M,i} - Q_{SF,i}\right)^2}{\sum_{i=1}^{N} \left(Q_{M,i} - \overline{Q_M}\right)^2} \qquad \text{Equation 2}$$

$$B_R = \frac{Q_{SF} - Q_M}{Q_{SF}}; \quad B_{RO} = \frac{Q_{SF} - Q_{SO}}{Q_{SF}}; \quad B_{R1} = \frac{Q_{SO} - Q_M}{Q_{SO}} \qquad \text{Equation 3}$$

Both indicators were not only applied to describe the goodness of fit between forecasted and observed flow ($Q_{SF}/Q_{M)}$ but as well for describing the fit between Q_{SF}/Q_{SO} and Q_{S0}/Q_M. The model errors were checked for possible dependencies with regard to (a) forecast lead time and (b) the magnitude of the forecasted discharge.

3 Results

Figure 2 shows the uncorrected precipitation cumulated during different forecast horizons T_F. For every nominal forecast time T_0 the total rainfall (from observation and INCA) within the forecast lead time T_F is plotted. The event on 03 June 2010 is an example where the later observed rainfall was forecasted well. In contrast in the beginning of the time window, forecast rainfall was overestimated. 48 hours forecast sums are met as good as sums for smaller forecast lead times up to 6 hours.

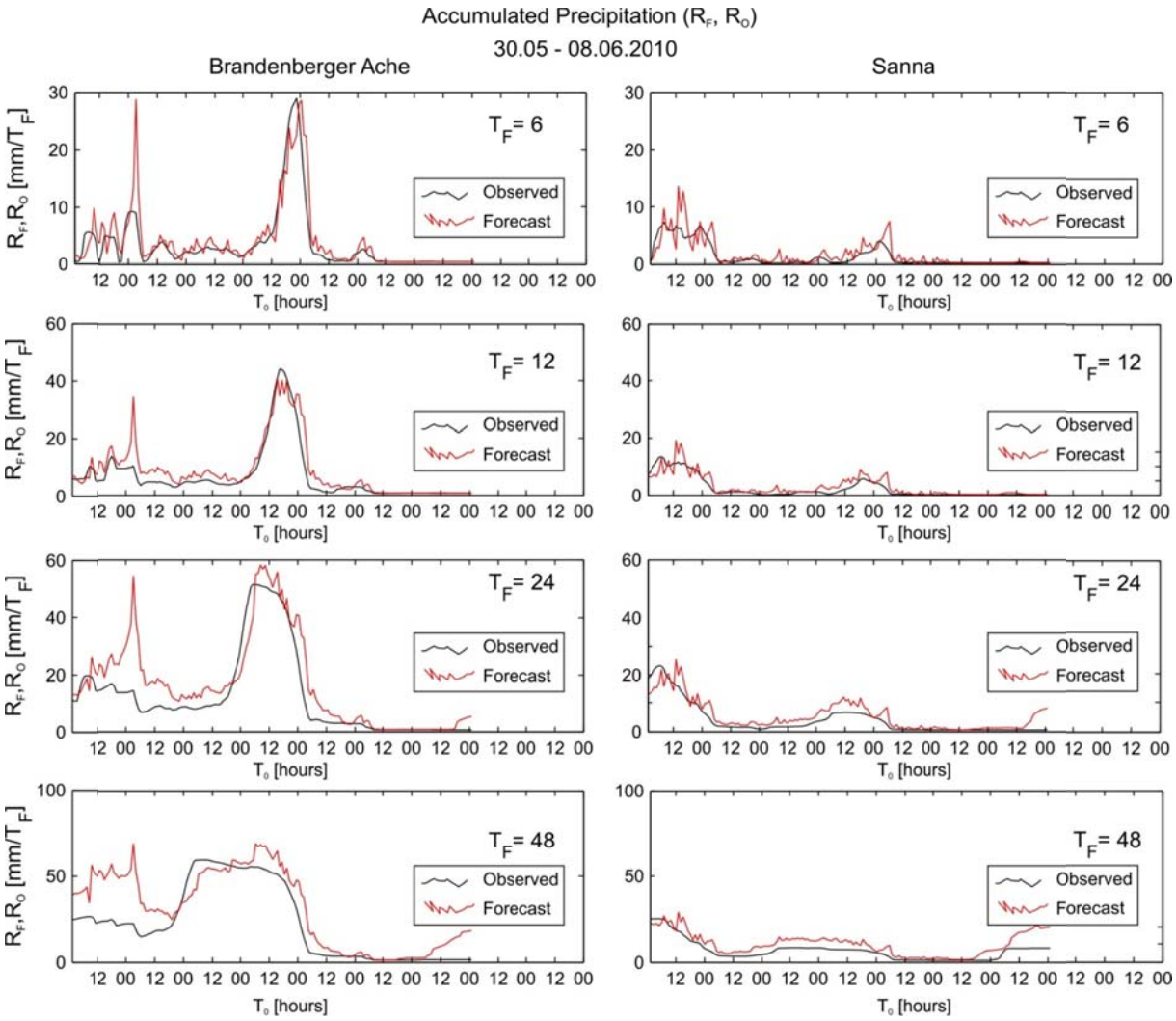

Figure 2: Comparison of rainfall accumulated at different forecast lead times T_F in the Brandenberger Ache and Sanna catchments (Event: 03. June 2010).

Figure 2 also shows the variability of the impact of particular weather conditions on different subcatchments within the Inn catchment. The well forecasted rainfall leads to – as expected – a good forecast of discharges for the Brixentaler Ache and Brandenberger Ache catchments (Figure 3). The top row shows the hydrographs of observed (blue) simulated (black) and forecasted (red) discharges for the full forecast horizon of 48 hours. The Nash Suttcliffe Efficiency (NSE) between the runoff, simulated based on observed data (Q_{SO}) and observed discharge (Q_M) was calculated for the entire event period (30.05.2010 – 08.06.2010). The obtained NSE of 0.86 and 0.84 for the two catchments indicates a well calibrated model.

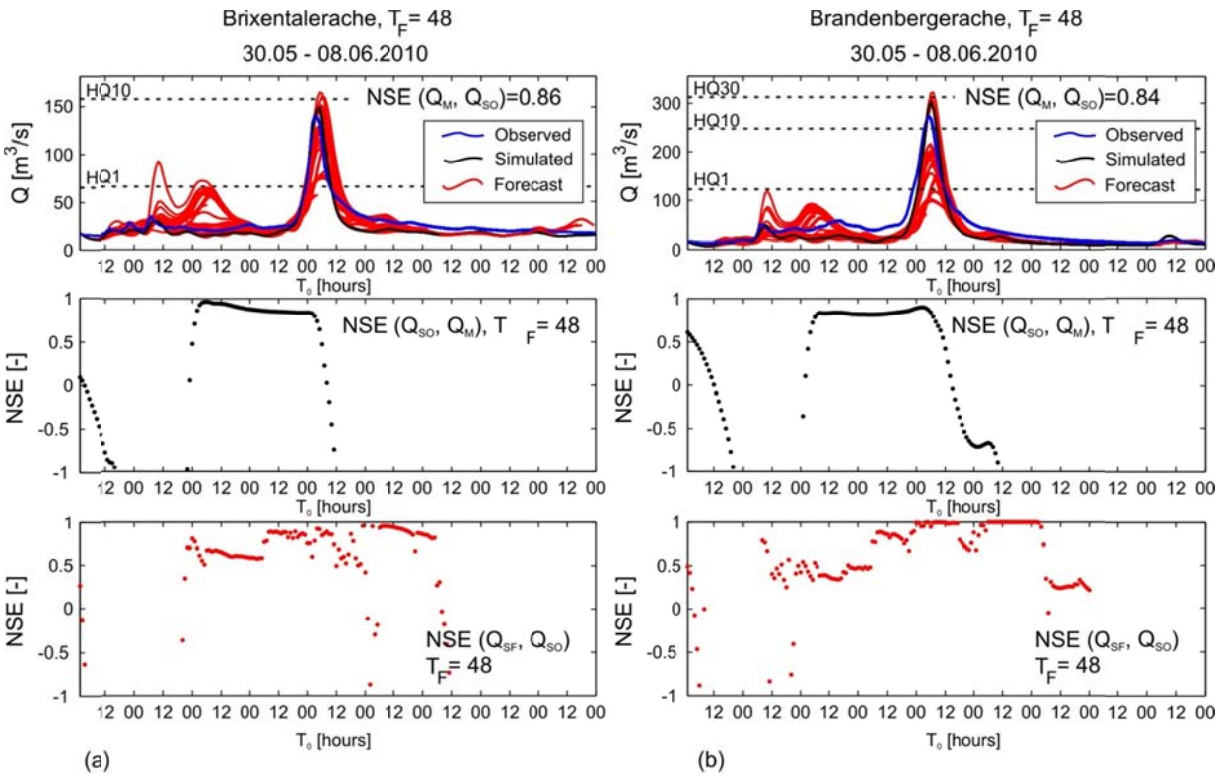

Figure 3: Storm event 30th May 2010 at (a) the Brixentaler Ache and (b) the Brandenberger Ache catchments. Hydrograph of observed (blue) simulated (black) and forecasted (red) discharge. NSE are plotted for all forecasts relating Q_{SO}/Q_M and Q_{SF}/Q_{SO} respectively.

The NSE in the second row represents the NSE between the runoff, simulated based on observed data (Q_{SO}) and observed discharge (Q_M), but calculated for each forecast period (T_F) separately. Thus, each point represents the NSE between Q_{SO} and Q_M for the next 48 hours. The NSE's of periods including the rising limb are close to the optimum value of 1. In contrast the NSE values are significantly less before the rising limb and after the peak. Still the hydrograph plots indicate a good visual fit as well. This is partly attributable to the fact that NSE is not suitable as an indicator for time series with small gradients and/or systematic errors (a flat hydrograph and slight underestimation in this case). Further, the NSE between forecasted (Q_{SF}) and simulated discharge (Q_{SO}) is also calculated, indicating a good fit of forecast hydrographs during the event as well.

In Figure 4 the hydrographs of two events ((a) 05.07.2009 and (b) 14.07.2009) are shown, illustrating large errors introduced by (a) the forecasted rainfall data and (b) the uncorrected observed rainfall data. In both cases the discharges are overestimated.

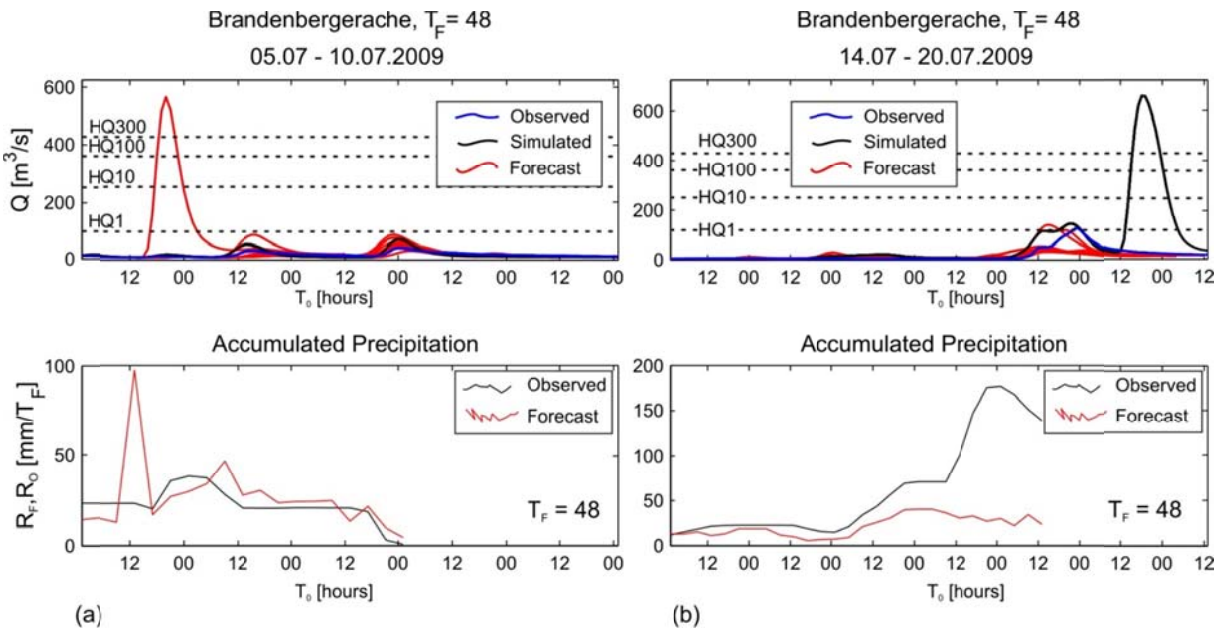

Figure 4: Evaluation of discharge in the Brandenberger Ache catchment of (a) 05.07.2009 and (b) 14.07.2009 showing the influence of errors in the rainfall forecast and observed rainfall on simulated discharge, respectively.

The scatter plots of modelled and observed discharges shown in Figures 5, 6 and 7 grant an insight on the range of errors (including all outliers) for the catchments Brandenberger Ache, Sanna and Ötztal. The discharges of all 14 events are plotted, regardless of the forecast lead time. In order to allow a differentiation of error source inherent in rainfall forecast and rainfall observation, three different scatter plots are compiled. The top left scatterplot (a) shows runoff, simulated based on forecasted meteorological data (Q_{SF}) plotted against observed discharge (Q_M). This plot allows to assess the overall performance of forecasted discharge including both, model- and input errors, assuming that the observed discharge (Q_M) is not affected by measuring errors. The plots (b) comparing the runoff, simulated based on meteorological observations (Q_{So}) against the observed discharge (Q_M) can indicate potential model- and/or calibration errors. Finally the plots (c), showing the runoff, simulated based on observed data (Q_{So}) against the runoff, simulated based on forecasted data (Q_{SF}), allow to visually assess the error caused by the quality of meteorological forecasts.

For the case of Brandenberger Ache shown in Figure 5, the underestimations in the discharge forecast can be attributed to the forecasting error of precipitation. The large overestimation of discharge is mainly due to artefacts in the rainfall

observations (see Figure 4) and originates only in some cases from erroneous precipitation forecasts. Box plot (b) in Figure 5, plotting Q_{SO} against Q_M indicates an overestimation of smaller flood events by the model. However large events, which are most relevant for flood warning, are simulated reasonably well.

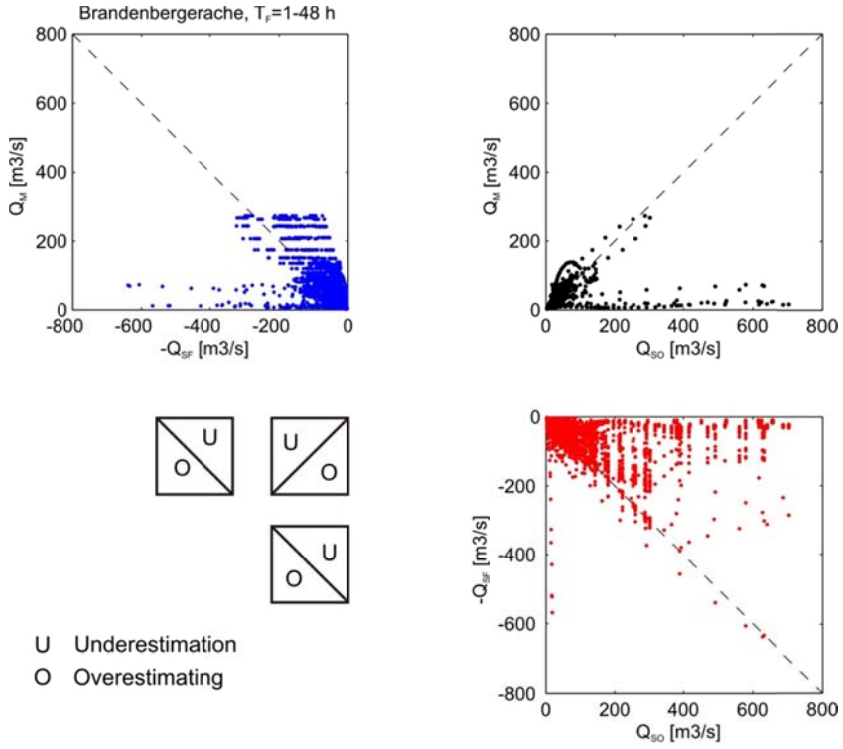

Figure 5: Brandenberger Ache: Scatter plots of discharge (a) forecast (Q_{SF}) vs. observed (Q_M) (b) simulated (Q_{SO}) vs. observed (Q_M) and (c) simulated (Q_{SO}) vs. forecast (Q_{SF}) discharge.

In Figure 6, the same types of scatter plots are shown for the Sanna catchment. Over- and under-estimations still occur, but not to such an extent as for Brandenberger Ache. Overall, the total error bandwidth is attributable to forecast errors and to a lesser extent of errors in observed rainfall. A similar effect can be observed for the largest tributary catchment, the Ötztaler Ache (Figure 7).

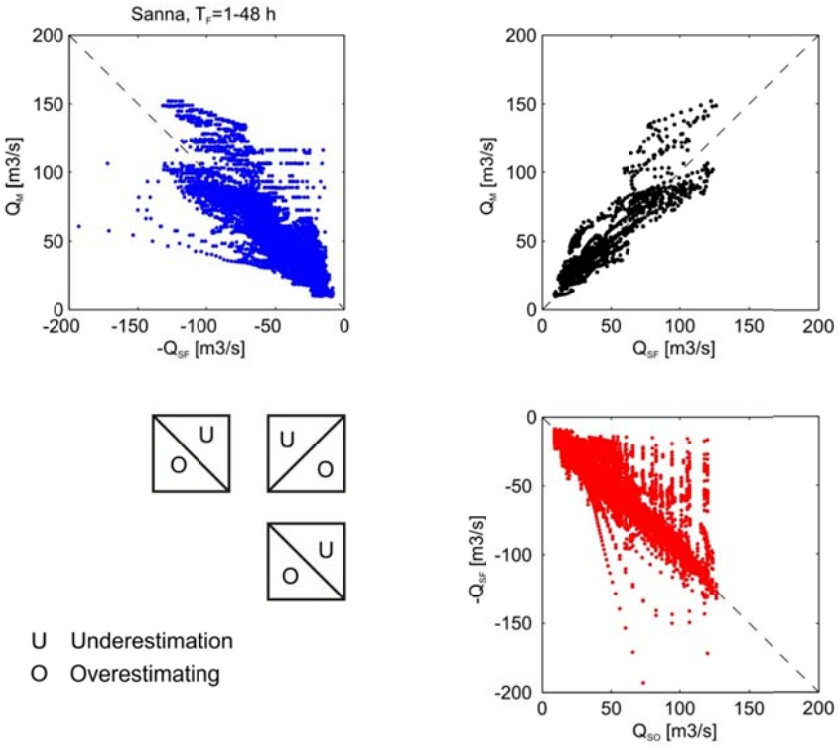

Figure 6: Sanna catchment: Scatter plots of discharge (a) forecast (Q_{SF}) vs. observed (Q_M) (b) simulated (Q_{SO}) vs. observed (Q_M) and (c) simulated (Q_{SO}) vs. forecast (Q_{SF}) discharge.

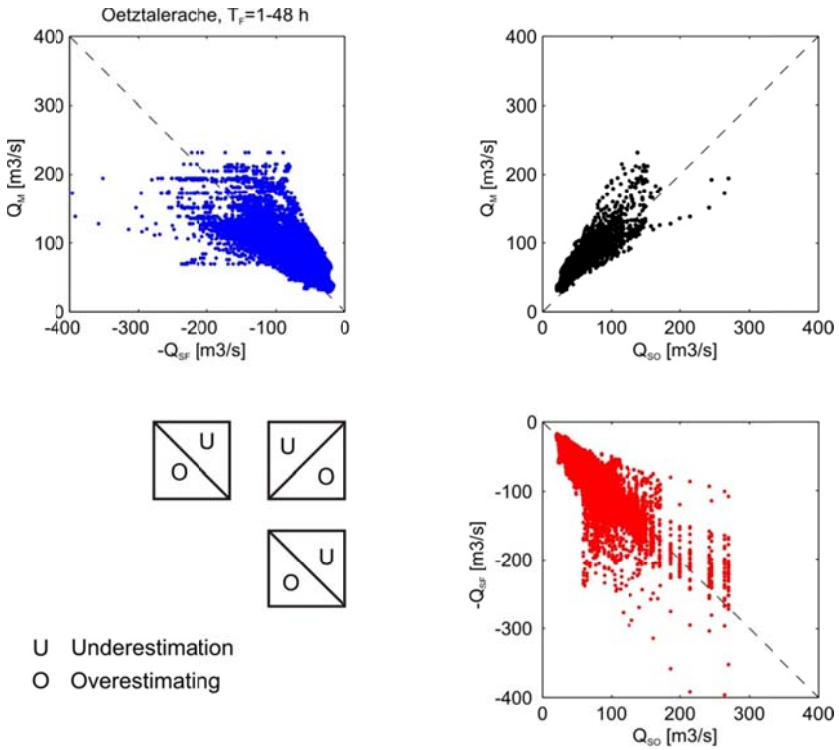

Figure 7: Ötztaler Ache catchment: Scatter plots of discharge (a) forecast (Q_{SF}) vs. observed (Q_M) (b) simulated (Q_{SO}) vs. observed (Q_M) and (c) simulated (Q_{SO}) vs. forecast (Q_{SF}) discharge

Figures 8, 9 and 10 show the evaluation of forecast and simulation errors with regard to the forecast lead time (plots on the left) and with regard to the forecasted discharge level or flood magnitude (plots on the right). The relative bias B_R (Equation 3) was used as an indicator to describe the error between runoff, simulated based on forecasted data (Q_{SF}) and observed discharge (Q_M) (top plots).This plot allows to assess the change of total error of forecasted discharge due to both model- and input errors depending on the forecast lead time or flood magnitude, respectively. The relative bias B_{R0} (mid plots) accounts for the error between runoff, simulated based on forecasted (Q_{SF}) and runoff, simulated based on observed meteorological data (Q_{So}). Errors which are visible in this plot are due to the deviation between meteorological observations and forecasts. Finally, the relative bias B_{R1} represents the error between runoff, simulated based on meteorological observations (Q_{So}) and measured discharge (Q_M). From this plot the error in the model itself and its calibration or input error is visible. A plot of the relative bias B_{R1} against the forecast lead time is excluded since there is no physically meaningful dependency between the variables. In order to quantify the magnitude of the forecasted discharge, the design discharges for different recurrence intervals are included in the plots.

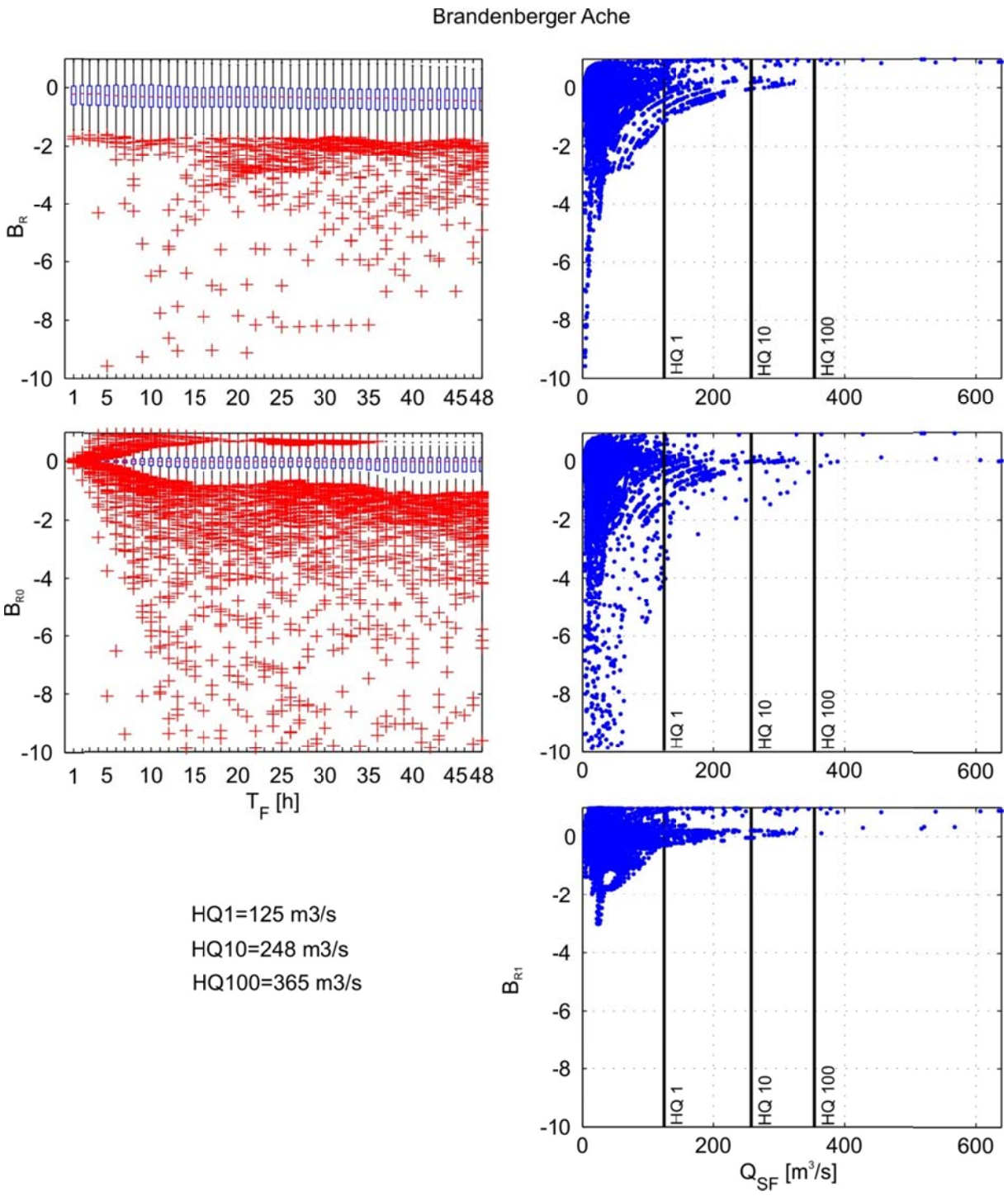

Figure 8: Brandenberger Ache Catchment: Plots of the relative bias (B_R, B_{R0} and B_{R1}) versus forecast lead time T_F (left) and versus the forecast discharge (Q_{SF}) (right).

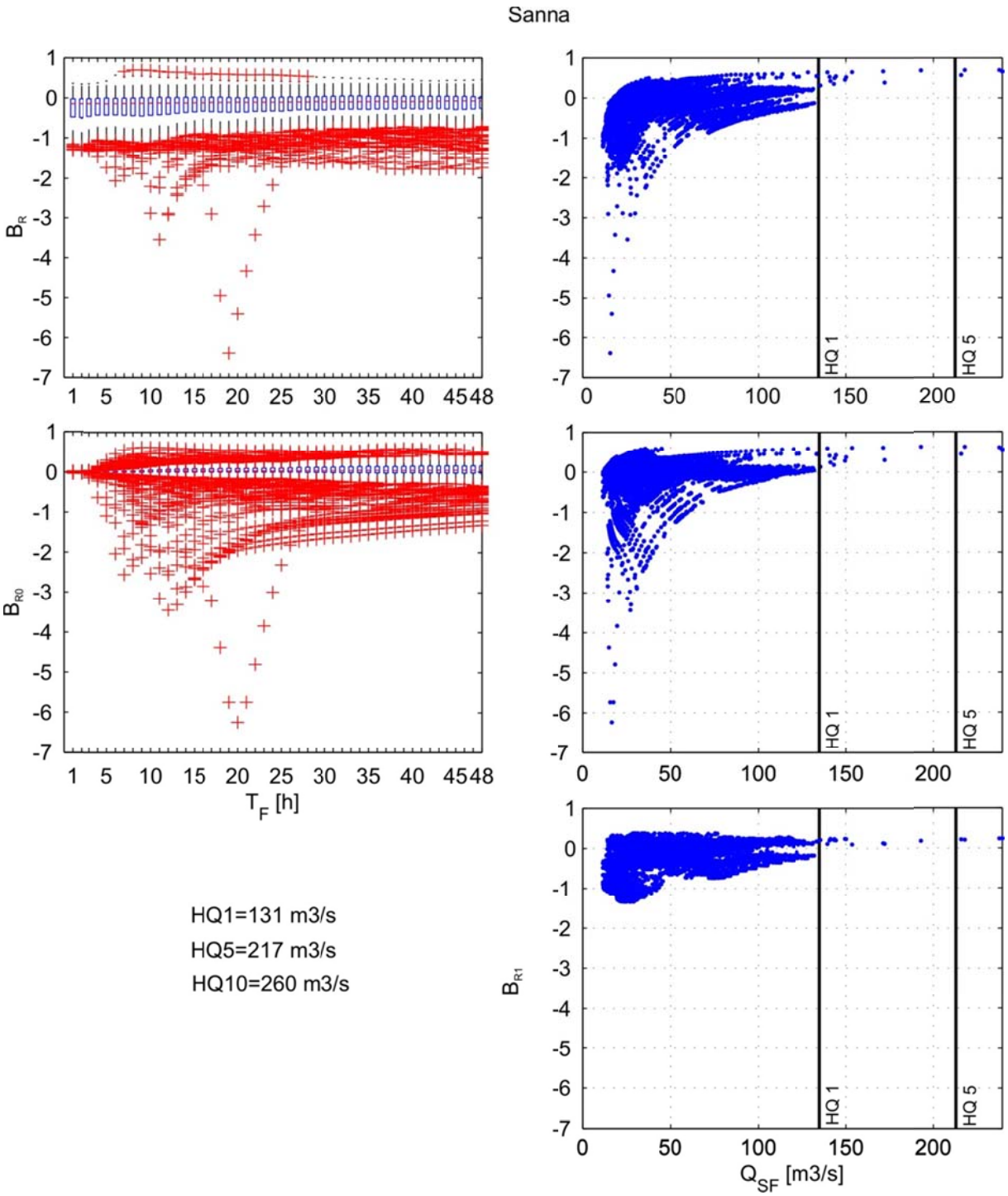

Figure 9: Sanna Catchment: Plots of the relative bias (B_R, B_{R0} and B_{R1}) versus forecast lead time T_F (left) and versus the forecast discharge (Q_{SF}) (right).

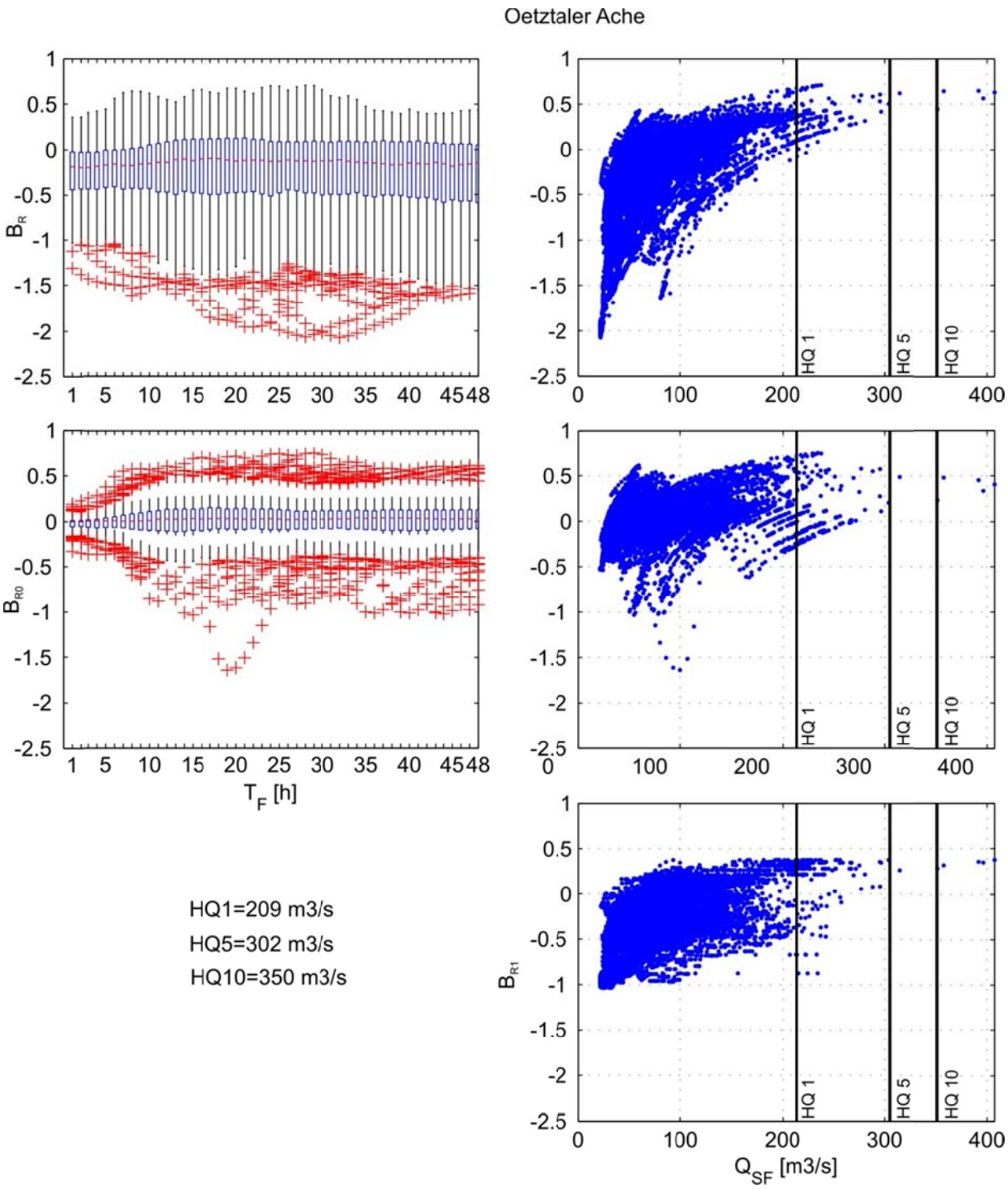

Figure 10: Ötztal Catchment: Plots of the relative bias (B_R, B_{R0} and B_{R1}) versus forecast lead time T_F (left) and versus the forecast discharge (Q_{SF}) (right).

All the catchments show a more or less wide spread range of errors when single outliers are considered. Still, the mean relative bias (having its optimum at zero), indicates good results in the mean with a certain error bandwidth considered as the standard deviation in the presented box plots.

4 Conclusion and Outlook

The presented analysis shows the range of possible errors in the hydrological models of a forecasting system under operational boundary conditions. No model output correction of any kind was used in this investigation since the focus was on quantifying the forecasting performance of the hydrological models alone. In all simulation runs, observed and forecasted input data was used as obtained during the online operation of the forecasting system. A known drawback is the limited checks on the erroneous precipitation measurements obtained online before they are applied within the flood forecast simulations. This leads to data uncertainty not only in the forecasted meteorological data but also in the observed meteorological data itself.

Still, within all four of the investigated tributary catchments of the river Inn, different examples were found for very well forecasted events (e.g. Figure 3) and poorly forecasted events (e.g. Figure 4) likewise. Figures 5, 6 and 7 give an overview on the deviations between measured, forecasted and simulated flow (Q_M, Q_{SF} and Q_{SO}) including even extreme outliers. The plots reveal that errors originate from the uncertain forecast input. Still, large errors originating from the simulation with observed precipitation can be the case. This is illustrated in Figure 5 where Q_{SO} is plotted versus Q_M in the case of the Brandenberger Ache catchment.

The simulations were further investigated for error magnitudes linked to either the forecast lead time T_F or the forecasted discharge quantity Q_{SF}. A tendency of decreasing errors with decreasing forecast lead time T_F as observed for the rainfall forecast used (Haiden et al., 2010) could not be found for the simulated discharges. Considering the concentration times shown in Table 1, it can be clearly seen that observed meteorological inputs contribute to the discharge during the first hours of the forecast lead time. Thus, the observed precipitation and the associated errors contribute as well in the forecast period and eliminate a possible reduced error level in the first hours after T_0. The fact that there is no dependency of error levels to the forecast horizon can also be found in the work of Blöschl et al. (2008) when using modeling approaches with no update of the model states. In the lead time depended plot, the mean observed relative bias (B_R) was found to be -0.20 for the Sanna and Ötztaler Ache catchments and -0.25 for the Brandenberger Ache catchment. This is slightly higher but still in the range of the mean errors presented by Blöschl et al.

(2008). The largest standard deviation was found to be between 0 and -0.5 for the case of the Ötztaler Ache catchment.

The right hand side plots of figures 8, 9 and 10 show the plots of relative bias against the discharge forecast magnitudes. In all cases, a significant reduction of the spread of the relative bias can be seen with an increasing discharge. The error reduction with increasing discharges meets the focus of a flood forecasting system. Still, the total error is a combination of errors originating in the forecasted and in the observed precipitation.

Current practice is to verify the results by expert judgement. Doing so, regularly extreme artifacts in observed precipitation have to be expected and excluded in a recalculation of the forecast. The current operational routines of the forecast system involve already a simple model output correction. Still, the ability of a significant error reduction, specially the reduction of outliers due to poorly observed rainfall, has been recognized to be a serious problem. Currently no routines for updating initial states of the models are implemented. Still, based on experiences from other authors (eg. Blöschl et al. (2008)), the implementation of model state updating routines is seen as an promising option to further improve the forecasting quality.

5 Acknowledgements

This work has been realized under the alpS Project “HoPI II - Flood Forecasting System for the Tyrolean Inn - A hybrid hydraulic/hydrologic model for improving flood forecasts”. The authors would like to thank the federal state of Tyrol, Austrian Research Promotion Agency (FFG) and the TIWAG - Tiroler Wasserkraft AG, who support the project.

6 Literature

Achleitner, S., Rinderer, M., Kirnbauer, R., 2009. Hydrological modeling in alpine catchments: sensing the critical parameters towards an efficient model calibration. Water Sci Technol, 60(6): 1507-1514.

Arheimer, B., Lindstrom, G., Olsson, J., 2010. A systematic review of sensitivities in the Swedish flood-forecasting system. Atmospheric Research, In Press(Corrected Proof).

Asztalos, J., 2004. Ein Schnee- und Eisschmelzmodell für vergletscherte Einzugsgebiete (Master Thesis), Institute for Hydraulic and Water Resources Engineering, Vienna University of Technology, Austria.

Asztalos, J., Kirnbauer, R., Escher-Vetter, H., Ludwig, B., 2007. A distributed energy balance snow and glacier melt model as a component of a flood forecasting system for the Inn river. , Alpine Snow Workshop. Berchtesgaden National Park research report, Nr.53, Munich, Germany, pp. 9-17.

Blöschl, G., Gutknecht, D., Kirnbauer, R., 1991a. Distributed Snowmelt Simulations in an Alpine Catchment .2. Parameter Study and Model Predictions. Water Resources Research, 27(12): 3181-3188.

Blöschl, G., Kirnbauer, R., Gutknecht, D., 1991b. Distributed Snowmelt Simulations in an Alpine Catchment .1. Model Evaluation on the Basis of Snow Cover Patterns. Water Resources Research, 27(12): 3171-3179.

Blöschl, G., Reszler, C., Komma, J., 2008. A spatially distributed flash flood forecasting model. Environ Modell Softw, 23(4): 464-478.

BMLFUW, 2007. Hydrologischer Atlas Österreichs (HAÖ), BMLFUW, Abt. VII 3 Hydrographisches Zentralbüro, Vienna, Austria.

Bossard, M., Feranec, J., Otahel, J., 2000. CORINE Land Cover - Technical Guide, Technical report No 40, 105 pp.

Braun, L., 1985. Simulation of snowmelt-runoff in lowland and lower alpine regions of

Switzerland. Zürcher Geographische Schriften, 21, 166 pp.

Dozier, J., Marks, D., 1987. Snow mapping and classification from landsat thematic mapper data. Annals of Glaciology, 9: 97-103.

Ehret, U. et al., 2009. Operational hydrological forecasting in Bavaria. Part I: Forecast uncertainty. Geophysical Research Abstracts, EGU General Assembly 2009, 11(EGU2009-13204).

Golding, B.W., 1998. Nimrod: A system for generating automated very short range forecasts. Meteorol. Appl., 5: 1-16.

Golding, B.W., 2000. Quantitative precipitation forecasting in the UK. Journal of Hydrology, 239: 286-305.

Haiden, T., Kann, A., Stadlbacher, K., Steinheimer, M., Wittmann, C., 2010. Integrated Nowcasting Through Comprehensive Analysis (INCA) – System Overview, ZAMG, Central Institute for Meteorology and Geodynamics, Vienna, Austria.

Hall, D.K., Riggs, G.A., Salomonson, V.V., 1995. Development of Methods for Mapping Global Snow Cover Using Moderate Resolution Imaging Spectroradiometer Data. Remote Sens Environ, 54(2): 127-140.

Hamon, R.W., 1963. Computation of Direct Runoff Amounts From Storm Rainfall, International Association of Scientific Hydrology, Wallingford, Oxon., U.K., pp. 52-62.

Hock, R., 1999. A distributed temperature index ice and snow melt model including potential direct solar radiation. Journal of Glaciology 45(149): 101-111.

Jasper, K., Gurtz, J., Herbert, L., 2002. Advanced flood forecasting in Alpine watersheds by coupling meteorological observations and forecasts with a distributed hydrological model. Journal of Hydrology, 267(1-2): 40-52.

Kasten, F., Czeplak, G., 1980. Solar and Terrestrial-Radiation Dependent on the Amount and Type of Cloud. Sol Energy, 24(2): 177-189.

Kleindienst, H., 1996. Erweiterung und Erprobung eines anwendungsorientierten hydrologischen Modells zur Gangliniensimulation in kleinen Wildbacheinzugsgebieten, Ludwig Maximilians University Munich.

Komma, J., Reszler, C., Bloschl, G., Haiden, T., 2007. Ensemble prediction of floods - catchment non-linearity and forecast probabilities. Natural Hazards and Earth System Sciences, 7(4): 431-444.

Marchi, L., Borga, M., Preciso, E., Gaume, E., 2010. Characterisation of selected extreme flash floods in Europe and implications for flood risk management. Journal of Hydrology, 394(1-2): 118-133.

Morgali, J., Linsley, R., 1965. Computer analysis of overland flow. Journal of Hydraulics Division, American Society of Civil Engineers, 91(3): 81-100.

Nash, J., 1960. A unit hydrograph study with particular reference to British catchments. Proceedings, Institution of Civil Engineers, 17: 249–282.

Nash, J.E., Sutcliffe, J.V., 1970. River flow forecasting through conceptual models, Part I - A discussion of principles. Journal of Hydrology, 10: 282-290.

Reichel, G., Fäh, R., Baumhackl, G., 2000. FLORIS-2000: Ansätze zur 1.5D-Simulation des Sedimenttransportes im Rahmen der mathematischen Modellierung von Fließvorgängen. In: Heigerth, G. (Ed.), Symposium: Betrieb und Überwachung wasserbaulicher Anlagen, Graz, 19. - 20.10.2000. Inst. f. Wasserbau u. Wasserwirtschaft, Techn. Univ. Graz, pp. 485-494.

Rickenmann, D., 1996. Fließgeschwindigkeit in Wildbächen und Gebirgsflüssen. Wasser-Energie-Luft 88(11/12): 298-303.

Rinderer, M., Achleitner, S., Asztalos, J., Kirnbauer, R., 2008. Sensitivity analysis of laps rate and corresponding elevation of snowline – limited data availability and its impact on snow and glacier melt. In: Institute for Catastrophic Loss Reduction (Ed.), 4th International Symposium on Flood Defence, 5th - 8th May 2008, Toronto, Canada.

Rossa, A. et al., 2010a. The COST 731 Action:next term A Review on Uncertainty Propagation in Advanced Hydro-meteorological Forecast. Atmospheric Research (in press).

Rossa, A.M. et al., 2010b. Radar-driven high-resolution hydro-meteorological forecasts of the 26 September 2007 Venice flash flood. Journal of Hydrology, 394(1-2): 230-244.

Schöber, J., Achleitner, S., Kirnbauer, R., Schöberl, F., Schönlaub, H., 2010a. Hydrological modelling of glacierized catchments focussing on the validation of simulated snow patterns – applications within the flood forecasting system of the Tyrolean river Inn. Adv. Geosci., 27: 99-109.

Schöber, J., Achleitner, S., Kirnbauer, R., Schöberl, F., Schönlaub, H., 2010b. Impact of model state selection for the flood formation in glacierized catchments In: Syme, G. (Ed.), Hydrology Conference Elsevier, San Diego, California.

Trofimova, E., 1970. Metod rascheta otrazhayushchej sposobnosti snezhnogo pokrova (A method for the calculation of the Reflectance characteristics of snow surfaces). Sredneaziatskij Nauchno Isseledovatelskij Gidrometeorologicheskij Institut, Leningrad, 52(67): 21-25.

US Army Corps of Engineers, 1956. Snow hydrology, Summary report of the snow investigations, North Pacific Division, Portland (Oregon).

van Genuchten, Mualem, 1980. A closed-form equation for predicting the hydraulic conductivity of unsaturated soils. Soil Science Society of America Journal, 44: 892–898.

Verbunt, M., Walser, A., Gurtz, J., Montani, A., Schar, C., 2007. Probabilistic flood forecasting with a limited-area ensemble prediction system: Selected case studies. J Hydrometeorol, 8(4): 897-909.

Wang, Y., Haiden, T., Kann, A., 2006. The operational limited area modelling system at ZAMG: Aladin-Austria. Österreichische Beiträge zu Meteorologie und Geophysik, 37: 33.